Effect of terrestrial nutrient limitation on the estimation of the remaining carbon budget

Makcim De Sisto [1,2] and Andrew H. MacDougall [1]

[1]Climate and Environment, St. Francis Xavier University, Antigonish, NS, Canada
[2]Faculty of Engineering and Applied Science, Memorial University of Newfoundland, NL, Canada

Correspondence: Makcim De Sisto (mdesisto@stfx.ca)

Abstract.

The carbon cycle plays a foundational role in the estimation of the remaining carbon budget. It is intrinsic for the determination of the transient climate response to cumulative CO_2 emissions and the zero emissions commitment. For the terrestrial carbon cycle, nutrient limitation has a core regulation on the amount of carbon fixed by terrestrial vegetation. Hence, the addition of nutrients such as nitrogen and phosphorus in land model structures in Earth system models is essential for an accurate representation of the carbon cycle feedback in future climate projections. Thereby, the estimation of the remaining carbon budget is impacted by the representation of nutrient limitation in modelled terrestrial ecosystems, yet it is rarely accounted for. Here, we estimate the carbon budget and remaining carbon budget of a nutrient limited Earth system model, using nitrogen and phosphorus cycles to limit vegetation productivity and biomass. We use eight shared socioeconomic pathways scenarios and idealized experiments on three distinct model structures: 1) carbon cycle without nutrient limitation, 2) carbon cycle with terrestrial nitrogen limitation and 3) carbon cycle with terrestrial nitrogen and phosphorus limitation. To capture the uncertainty of the remaining carbon budget, three different climate sensitives were tuned for each model version. Our results show that overall the nutrient limitation reduced the remaining carbon budget for all simulations in comparison with the carbon cycle without nutrient limitation. Between the nitrogen and nitrogen-phosphorus limitation, the latter had the lowest remaining carbon budget. The mean remaining carbon budget from the Shared Socioeconomic Pathways scenarios simulations for the 1.5 °C target in the no nutrient limitation, nitrogen limited and nitrogen-phosphorus limited models obtained were 228, 185 and 175 Pg C respectively, relative to year 2020. For the 2 °C target the mean remaining carbon budget were 471, 373 and 351 Pg C for the no nutrient limitation, nitrogen limited and nitrogen-phosphorus limited models respectively, relative to year 2020. This represents a reduction of 19 and 24 % for the 1.5 °C target and 21 and 26 % for the 2 °C target in the nitrogen and nitrogen-phosphorus limited simulations compared to the no nutrient limitation model. These results show that terrestrial nutrient limitations constitute an important factor to be considered when estimating or interpreting remaining carbon budgets and are an essential uncertainty of remaining carbon budgets from Earth system model simulations.

1 Introduction

Nutrient availability constrains the capacity and rate at which terrestrial plants assimilate carbon (Goll et al. , 2012). Nitrogen and phosphorus are the nutrients that most commonly limit vegetation growth (Filipelli , 2002; Fowler et al. , 2013; Wang et al. , 2010; Du et al. , 2020) and hence have been the subject of most research and large scale modelling efforts. Globally, this effect varies. Most of the terrestrial biosphere is co-limited by both N and P, with N being the dominant nutrient limitation in higher latitudes while phosphorus predominates in lower latitudes (Du et al. , 2020). Earth system models are designed to account for land use change, and biological productivity when estimating the carbon sink on land (Kiwamiya , 2020). The change of nutrient concentration in terrestrial systems in future simulations is an uncertainty for determining the land carbon sink over the next decades (Shibata et al. , 2010, 2015; Menge et al. , 2012). Complicating this problem further, a large portion of nutrients on land are derived from anthropogenic sources, including agricultural fertilization (artificial, compost and manure), atmospheric deposition of N-bearing pollutants, and urban wastewaters (Lu and Tian , 2017; van Puijenbroek et al. , 2019).

Future climate projections have only rarely accounted for nutrient limitation of the land carbon sink (Wang and Goll , 2021). For the sixth phase of the Coupled Model Intercomparison Project (CMIP6) this weakness was partially overcome with more Earth system models (ESMs) embracing nitrogen limitation as a standard for terrestrial system structures. However, the inclusion of phosphorus remains rare and representation of micro-nutrients remains a distant ambition. (Arora et al. , 2020; Spafford and MacDougall , 2020). Thus, the future of the land carbon sink remains uncertain as projecting the interactions between the terrestrial system and atmosphere is a challenge without fully accounting for nutrient limitations (Achad et al. , 2016). Since year 1850, the cumulative CO_2 land sink has been estimated to be 210±45 PgC, which represents 31% of all anthropogenic carbon emissions (Friedlingstein et al. , 2022). The terrestrial carbon sink has increased historically with increasing CO_2 emission rate, such that the proportion of carbon taken up by land has remained close to constant (Friedlingstein et al. , 2022).

It is likely that the first generation of ESMs simulations overestimated how much terrestrial ecosystems would respond to an increase in atmospheric CO_2 concentrations based on carbon only schemes (Wieder et al. , 2015). A large amount of terrestrial carbon uptake was predicted by those simulations, which would result in unrealistic nutrient requirements. For example, in a study by Wieder et al. (2015) ESMs with nitrogen and nitrogen–phosphorus limitation were projected to decrease net primary productivity by 19% and 25%. Hence, the implementation of nutrient limitation in ESMs has been shown to improve the representation of carbon uptake in land (Wang et al. , 2007, 2010; Goll et al. , 2017; De Sisto et al. , 2023), and thus will effect the carbon budget.

The remaining carbon budget describes how much CO_2 emissions can be allowed to be emitted to stay below global atmospheric temperature target goals, commonly 1.5 and 2 °C (IPCC , 2021). This metric is of utmost importance for policy and emission reduction regulations. Therefore, the estimation of remaining carbon budgets and their uncertainties has led to numerous research efforts in the scientific community (e.g. Matthews et al. (2020); Lamboll et al. (2023)). The cumulative emission of CO_2 has been found to be nearly proportional to the change in global surface atmospheric temperatures (Tokarska et al. , 2018; Matthews et al. , 2020). This almost linear pattern can be conveniently used as a metric, the Transient Climate

Response to Cumulative CO_2 Emission (TCRE), to quantify how global surface temperatures change to cumulative CO_2 emissions (Matthews et al. , 2009; MacDougall , 2016; Spafford and MacDougall , 2020). The TCRE can then be applied to estimate remaining budgets, where its inverse represents the allowable carbon emitted for each temperature goal (Matthews et al. , 2020). This metric has been shown to be good for predicting the response of temperature to cumulative CO_2 emissions. However, the TCRE only represents warming from CO_2 emissions, excluding the impacts of non-CO_2 forcing agents. A method to account for this issue is to use the effective TCRE, which includes simulations with all anthropogenic forcings (Tokarska et al. , 2018).

As a metric, the TCRE has a large uncertainty within published research studies, ranging from 1.0 to 2.3 K EgC^{-1} (IPCC , 2021). Understanding the sources of these uncertainties can improve the estimation of remaining carbon budgets and thereby increase the accuracy of environmental regulations. For idealized experiments, the Transient Climate Response (TCR) can be used to quantify the physical uncertainty in TCRE. TCR is the amount of global warming expected to occur when atmospheric CO_2 concentrations double from their pre-industrial levels, while all other factors remain constant. This corresponds to year 70 in a 1pctCO2 experiment where the annual CO_2 concentration is increased at a rate of 1 % yr^{-1} (Eyring et al. , 2016). In Earth system models, the representation of the carbon cycle is one of the most important sources of uncertainties for the estimation of remaining carbon budgets (Matthews et al. , 2020).

Nutrient limitations play a vital role in the estimations of remaining carbon budgets due to their constrain on the terrestrial carbon cycle. This study assesses how nutrient limitation impacts several uncertainties in remaining carbon budget estimates, including uncertainty in the TCRE, the estimated contribution of non-CO_2 climate forcings to future warming, the correction for the feedback processes presently unrepresented by ESMs, and the unrealized warming from past CO_2 emissions–called the Zero Emissions Commitment (ZEC) (Rogelj et al. , 2018).

N and P are the main nutrients limiting terrestrial systems. Their inclusion of N and P in Earth system models has been shown to decrease the capacity of the land to uptake carbon and affect the vegetation biomass and distribution representation (Wang et al. , 2010; Goll et al. , 2017; Wang and Goll , 2021; De Sisto et al. , 2023). Aside from land sinking changes, terrestrial N and P limitation also impact land use change emissions and albedo due to decreased vegetation biomass (De Sisto et al. , 2023). Isolating the effects of N and P terrestrial limitation gives a novel insight into how underrepresented processes in terrestrial systems contribute to remaining carbon budget uncertainties. Hence, we explore the effect of terrestrial N and P limitation in remaining carbon budget estimates in an intermediate complexity ESM under historical, idealized, and Shared Socioeconomic Pathways projections.

2 Methodology

2.1 Model description

Simulations to quantify the remaining carbon budgets were carried with the University of Victoria Earth System Climate Model (UVic ESCM). The UVic ESCM version 2.10, is a global intermediate complexity model (Weaver et al. , 2001; Mengis et al. , 2020). The model is comprised of a 3D dynamic ocean circulation model (Pacanowski , 1995), along with a simplified moisture-energy balance atmosphere (Fanning and Weaver , 1996), a dynamic-thermodynamic sea ice model (Bitz et al. , 2001) and a land surface model (Meissner et al. , 2003).

In the model, the terrestrial and oceanic carbon cycle are represented. The ocean comprises 19 vertical levels that become thicker with depth (50 m near the surface to 500 m in the deep ocean). Ocean biogeochemistry is based on a simple nutrient-phytoplankton-zooplankton-detritus model (Keller et al., 2012; Schmittner et al., 2005), with representation of ocean carbonate chemistry and sediments (Mengis et al. , 2020).

In the 2.10 version of the model, the soil is represented by 14 subsurface layers with their thickness increasing exponentially with depth, with the surface layer measuring 0.1 m, the bottom layer measuring 104.4 m, and the total layer measuring 250 m. Hydrological processes are active in the first eight soil layers (top 10m), while the layers below have granitic characteristics. The soil carbon cycle is active up to a depth of 3.35 m (6 layers) (Avis , 2012; MacDougall et al. , 2012). TRIFFID (top-down representation of interactive foliage and flora including dynamics) represents vegetation interaction between 5 plant functional types (PFTs) within the terrestrial vegetation. Based on the Lotka-Volterra equations (Cox , 2001), broadleaf trees, needleleaf trees, shrubs, C3 grasses, and C4 grasses compete for space in the grid. Through photosynthesis, carbon is uptaken and allocated to growth and respiration, whereas the vegetation carbon is transferred to the soil through litter fall and allocated to the soil in a decreasing function of depth. Permafrost carbon is prognostically generated within the model using a diffusion-based scheme meant to approximate the process of cryoturbation (MacDougall and Knutti , 2016).

The UVic ESCM prescribes anthropogenic land-use changes based on standardized CMIP6 land-use forcing (Ma et al., 2020) regridded to the UVic ESCM grids. Land-use data products have been modified for UVic ESCM use by aggregating cropland and grazing land into one crop type, representing any of the five functional types of crops, and one grazing variable, representing pastures and rangelands. By using this forcing, the model determines the fraction of grid cells that contain crops and grazing areas, and these fractions are assigned to C3 and C4 grasses and excluded from the vegetation competition routine of TRIFFID. The dynamics of CO_2 emissions from land use change (LUC) are designed so that when forest or other vegetation are cleared for crop or pasture, 50 % of the tree carbon is released directly into the atmosphere, and the remaining is allocated into the litter pool. A full description of the model can be found in Mengis et al. (2020).

A terrestrial N and P modules has recently been developed for the UVic ESCM (De Sisto et al. , 2023). The N cycle module consists of three organic pools (litter, soil organic matter, and vegetation) and two inorganic pools (NH_4^+ and NO_3^-). Nitrogen input is represented by atmospheric nitrogen deposition and biological N fixation. The latter is dependent on the terrestrial Net Primary Productivity (NPP). Biological N fixation and mineralization of organic N produce NH_4^+, which can be absorbed by plants (vegetation), leached, or transformed into NO_3^- via nitrification. NO_3^- is produced through nitrification, can be taken up by plants, leached or denitrified into NO, N_2O or N_2. Inorganic N is distributed between leaf, root, and wood, with wood having a fixed stoichiometric ratio and leaf and root pools having a variable ratio. The partition of carbon, N and P among plant structures does not change in when the soil is considered to be nutrient limited. Organic N leaves the living pools via litter-fall into the litter pool which is either mineralized or transferred to the organic soil pool, part of this N can be mineralized into the inorganic N pools. Before litterfall, a constant 0.5 fraction of the N is reabsorbed. Mineralization of the litter and organic matter pool is dependent on turnover rates, concentration of N, soil temperature and soil moisture. At the same time N can flow from the inorganic to the soil organic pool via immobilization. A complete description of the N cycle can be found in Wania et al. (2012) and De Sisto et al. (2023).

The P module includes three inorganic (labile, sorbed and strongly sorbed) and three organic P pools: Vegetation (leaf, root and wood), litter and soil organic P. The P input is driven by a fixed estimates of P release per global soil types as in Wang et al. (2010). Inorganic P (P_{soil}) in soil follows the dynamics described in Goll et al. (2017) where a fraction of the inorganic soil P is transfered to the sorbed pool while the remaining fraction is consired to be labile. A portion of the sorbed pool is also transfered to the strong sorbed pool where it is considered a loss of phosphorus from the soil system. After uptake, P is distributed in three vegetation compartments: leaf, root and wood. Leaf and root have a dynamic value that varies between a minimum and a maximum, while wood have a fix C:P ratio. The vegetation P biomass dynamics are determined from the difference between the amount of uptake and the loss from litterfall. Before littefall, a 0.5 fraction of P is reabsorbed. The litter P pool is dependent on three terms: the input from litterfall, the decomposition rate and loss from mineralization (Wang et al. , 2007). The soil litter decomposed is transferred to the soil organic P pool. The mineralization of phosphorus is determined from the maximum rate of P mineralization, the N cost of plant root P uptake, a critical value of N cost for root P uptake from where phosphatase production begins and a Michaelis-Menten constant for P mineralization. A complete description of the P cycle can be found in De Sisto et al. (2023).

N and P limit terrestrial vegetation growth in the model in two different ways: 1) N limits the photosynthetical activity (by regulating the maximun carboxilation rate of RuBISCO) and directly by reducing biomass. This reduction is controlled by the maximum C:N leaf ratio, where reducing this value corresponds to a larger reduction of vegetation biomass. 2) A stoichiometric reduction of biomass when N and P are considered to be limiting terrestrial plants. If C:N ratios are above a set ratio threshold, wood and root carbon biomass are then transferred to the litter pool (reassembling decaying vegetation when in nutrient limiting environments) until the "normal" set C:N ratio is reached. There is no direct inclusion of P limitation in photosynthesis-related equations. Past model development efforts tested different approaches such as Walker et al. (2014) but the concepts were incompatible with the current version of land vegetation model structure.

2.2 Experimental set-up

The effects of N and P were analysed from the perspective of the sources of uncertainty in the remaining carbon budgets estimates. Here, the framework includes how N and P impact the representation of: 1) Model fidelity of human warming to date, 2) the TCRE, 3) the unrealized warming from past CO_2 emissions (zero emissions commitment) and, 4) the estimated contribution of non-CO_2 climate forcings to future warming. We run three different versions of the UVic ESCM version 2.10:

1) Carbon only (C-only), 2) Carbon Nitrogen (CN) and Carbon Nitrogen and Phosphorus (CNP). Furthermore, to capture the uncertainty of the carbon budget estimates, the equilibrium climate sensitivity was tuned by using a parameter designed by Zickfeld et al. (2009) to alter climate sensitivity in the UVic ESCM by altering the flow of long-wave radiation back to space. The dynamics of the alteration is represented in the following equation:

$$L^{*}_{out} = L_{out} - c(T - T_0), \tag{1}$$

where L^{*}_{out} is the modified longwave radiation, L_{out} is the unmodified longwave radiation, c is a proportionality constant that corresponds to specific equilibrium climate sensitivities, T is the present global average temperature and T_0 is the global average temperature at the initial year of the simulation. The parameter c is used to increase or decrease the net climate feedback by reducing or increasing the outgoing longwave radiation. Model variants were tuned to have Equilibrium Climate Sensitivities (ECSs) per doubling of CO_2 of 2.0°C, 4.5°C to represent the "likely bounds" (IPCC , 2021), as well as using the emergent climate sensitivity of the model (3.4°C) as the central estimate.

2.2.1 Historical human-induced warming to date

We conducted three historical simulations to assess the historical climate response differences between the C-only and CN and CNP. Each model structure was calibrated using aerosol scaling so that historical temperatures match observations. We used Goddard Institute for Space Studies (GISS) temperature observations in this study. Three-dimensional aerosol optical depth can be scaled by a fraction in the UVic ESCM and was used in version 2.10 to calibrate aerosol forcing to fit current values (Mengis et al. , 2020). Thus the historical warming to date is similar for all model variants but the estimated historical emissions vary, allowing model validation. The non-CO_2 forcing included solar, volcanic, aerosol and the aggregate forcing from halocarbons, CH_4, and N_2O.

2.2.2 Transient climate response to cumulative emissions

To diagnose the TCR and the TCRE, we run simulations starting with a 1% yr^{-1} increase in CO_2 concentrations until a doubling and quadrupling(2x and $4xCO_2$) were reached after which the concentration was kept constant (Eyring et al. , 2016). Both TCR and TCRE are computed at year 70 of this $1pctCO_2$ experiment, when atmospheric CO_2 concentration has doubled. To account for non-CO_2 forcing effect on climate sensitivity, we applied (Tokarska et al. , 2018) approach to compute effective TCRE. This approach uses Share Socioeconomic pathways (SSPs) projections to simulate a full forced simulation. The SSPs represent a range of possible futures, with each scenario defined by key characteristics. SSP1 reflects a sustainable and policy effective scenario where emissions are low and climate impact is minimized. SSP2 in a scenario with medium challenges for mitigation and adaptation. SSP3 is a high challenge for mitigation and adaption scenario. SSP4 is a low challenge for mitigation high challenge for adaption scenario. Finally, SSP5 is a high challenge for mitigation and low challenge for adaptaton scenario. For the effective TCRE, SSP 5-8.5 is used to represent a full forced simulation to estimate the response of temperature to cumulative emissions

2.2.3 Zero emissions commitment

To explore the effects of nutrient limitation on zero emission commitment, an experiment was done following the protocol of the Zero Emission Commitment Model Intercomparison Project (ZECMIP). The objective of ZECMIC is to quantify the amount of unrealized temperature change after CO_2 emissions have ceased and the drivers behind the change (Jones et al. , 2019). The experimental protocol was applied to C-only, CN and CNP. For these experiments the 1pctCO_2 experiment is followed until diagnosed cumulative emissions of CO_2 reaches 1000 PgC thereafter emissions are set to zero further CO_2 emissions. We diagnosed three emissions pathways corresponding to C-only, CN and CNP simulations. We used two metrics to assess the nutrient limitation effect on ZEC. The first, is the temperature at the 50th year after emission have ceased relative to the global average temperature when emissions ceased, averaged from year 40 to year 59 after emissions cease (ZEC_{50}) as in MacDougall et al. (2020). The second, is the mean ZEC for 100 years after emission have ceased.

2.2.4 Estimated effect of nutrient limitations on SSP scenario simulations

To estimate the impact of nutrient limitation on the contribution of non-CO_2 climate forcings to future warming, eight SSPs scenarios for the C-only, CN and CNP version of the UVic ESCM version 2.10 were run. We included the CMIP6 SSPs array scenarios representing each distinct future (1-5) narrative. The following scenarios were run: SSP1-1.9, SSP1-2.6, SSP2-4.5, SSP3-7.0, SSP4-3.4, SSP4-6.0, SSP5-3.4-OS and SSP5-8.5. The carbon budget follows temperature anomalies normalised to 1850-1900 mean for 1.5, 2, 2.5 and 3 °C targets. For the four overshoot scenarios (SSP1-1.9, SSP1-2.6, SSP4-3.4, and SSP5-3.4-OS) the remaining carbon budget is computed for the time when the target is first breached.

To estimate the effect of nutrient limitation on land use change emissions and terrestrial albedo an extra set of three simulations for C-only, CN and CNP and the same eight SSP scenario simulations where conducted. In these simulations land use change forcing was set to the pre-industrial year 1850 value. The model adjusts its diagnosed CO_2 emissions to account for the missing land use change forcing. Hence, the diagnosed emission difference between the simulations with land use change forcing and without forcing corresponds to the estimated amount of land use change emissions (Mengis et al. , 2018). These values also carry the effect of albedo change due to land use change. Hence, our values show the total land use change emission + albedo effect simulated in the model.

Table 1. Model simulations set-up with descriptions.

Simulations	**Type**	**Descriptions**
C-only	Nutrient-Concentration driven	Carbon only simulation
CN	Nutrient-Concentration driven	Carbon-nitrogen simulation (nitrogen limited)
CNP	Nutrient-Concentration driven	Carbon-nitrogen-phosphorus simulation (nitrogen-phosphorus limited)
SSPs	Future scenarios-Concentration driven	Shared Socioeconomic Pathways
Climate sensitivity	Climate sensitivity-Concentration driven	Longwave radiation flow modified to alter equilibrium climate sentivity
TCR and TCRE	1pct CO_2 experiment-Concentration driven	1 percent CO_2 increase experiment.
Effective TCRE	SSP5-8.5-Concentration driven	All forcing SSP5-8.5 scenario.
ZEC	Concentration driven & emission driven	Zero emission commitment experiments

3 Results

3.1 Historical human-induced warming to date

For each model structure the historical temperature was calibrated to match historical observations by altering the efficacy of aerosol forcing. Figure 1 shows the resulting near-surface air temperature anomalies for UVic ESCM C-only, CN, and CNP configurations after calibration relative to 1951-1980 climate normal. The temperature anomalies were plotted against GISS near surface air temperatures anomalies relative to 1951-1980 (GISTEMP Team , 2023). For the three different versions of the model the resulting calibrated simulations reproduced well the historical temperature trend when compared to GISS observations. As shown in De Sisto et al. (2023) without calibration the UVic ESCM CN and CNP have higher temperatures when compared to C-only, given that nutrients limit the capacity of the terrestrial system to take up atmospheric CO_2. That is, atmospheric CO_2 is higher given the same total emissions of CO_2. Between CN and CNP, CNP results in higher temperature response mainly as a result of tropical terrestrial nutrient limitation and extra phosphorus limitation in higher latitudes.

Figure 2 shows the historical global carbon cycle from 1850-2021 for C-only, CN and CNP. There are two main impacts of nutrient limitation on terrestrial systems: 1) reduction of the land carbon sink and 2) reduction of the land use change emissions. The reduction of the land carbon sink is related to the decrease of the photosynthetic capacity and the regulation of terrestrial vegetation biomass. This biomass reduction leads to the reduction of the land use change emissions, especially as N and P affects woody biomass greatly. The global reduction of carbon uptake increase the concentration of atmospheric CO_2 in emission driven simulations. Following this logic and given that concentration driven simulation have a set atmospheric CO_2 concentrations, the diagnosed emissions estimated in our simulations were reduced in CN and CNP compared to C-only. The model estimates less emissions to be necessary to keep the CO_2 concentration on track as less carbon is taken up from land. In order to be comparable to the latest carbon budget report out estimation of the historical carbon cycle follows carbon fluxes from 1850-2021 while the estimation of the remaining carbon budgets starts from the year 2020 following different future SSPs scenarios pathways. From 1850-2021 (Figure 2) the range of reduction in the CN and CNP nutrient limited simulations for the cummulative land carbon sink was 75 to 106 Pg C compared to C-only. The range of reduction for cummulative the land use change emission was 60 to 93 Pg C. Finally, the range of reduction of the cumulative carbon emissions diagnosed by the concentration driven simulations was 11 to 29 Pg C. The CNP cumulative fossil fuel CO_2 emissions of 483 PgC is within the value of 465±25 PgC given by Friedlingstein et al. (2022) while C-only and CN are slightly over the estimate with 501 and 512 PgC (Figure 2).

3.2 Transient climate response to cumulative CO_2 emissions

The TCR for doubling CO2 concentrations was 1.78, 1.79 and 1.79 °C in C-only, CN and CNP. These small differences are driven by albedo changes. Between CNP and CN, the albedo change has a small increase effect of 0.004 °C in CNP compared to CN (note the UVic ESCM lacks internal variability, so this very small difference is computable). The TCRE for C-only resulted in 1.74 K EgC^{-1} compared to CN 1.94 K EgC^{-1} and CNP 2.07 K EgC^{-1}. The TCRE values for all the simulations are within the range of 1 - 2.3 K EgC^{-1} given by the IPCC AR6 Summary for Policy Makers (IPCC, 2021). Under a 1%

atmospheric CO_2 increase per year experiment, terrestrial nutrient availability limits the capacity of terrestrial vegetation to take up carbon. Hence, even with a rapid increase of CO_2 concentration in the atmosphere, terrestrial vegetation carbon uptake capacity is limited, and the uptake rates are not as high as with an unlimited amount of nutrients readily available for uptake. The effective TCRE estimated from SSP5-8.5 resulted in 1.97, 2.27 and 2.36 K EgC $^{-1}$ for C-only, CN and CNP. Overall the TCRE and effective TCRE were increased in the nutrient limited simulations. The range of increase for TCRE was: 0.2 to 0.3 K EgC $^{-1}$. The range of increase of the effective TCRE was: 0.3 to 0.4 K EgC $^{-1}$. Figure 2 shows how terrestrial carbon cycle fluxes change in historical simulations. Due to these changes the diagnosed CO_2 emissions are reduced, hence, for any temperature target less CO_2 emissions need to be emitted in the nutrient limited simulations. This translates into a more sensitive model, where for 1000Pg C emitted the nutrient limiting simulations are going to result in higher temperatures.

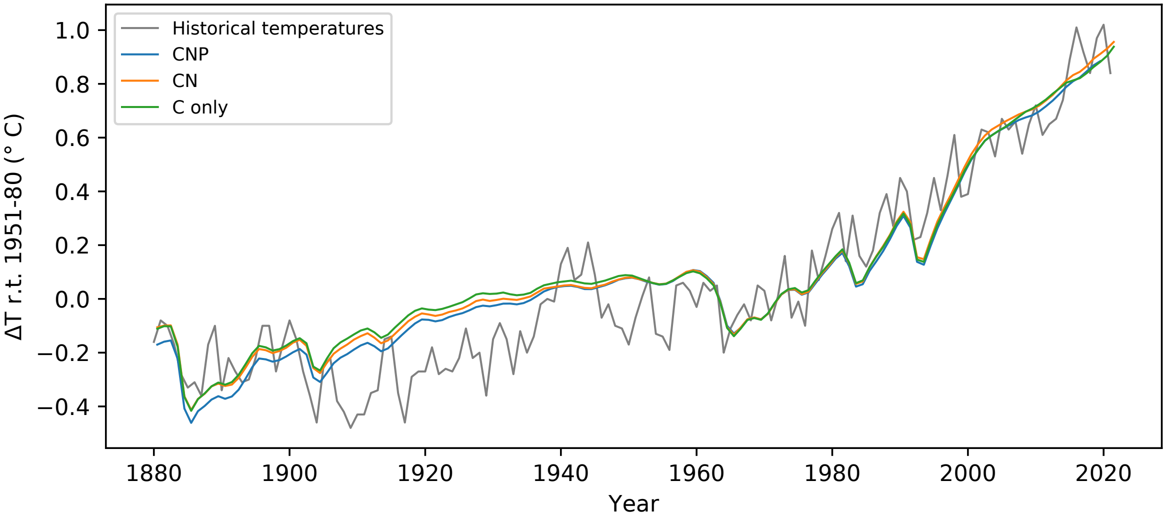

Figure 1. Historical temperature relative to 1951-1980 of C-only, CN and CNP compared to GISS historical temperature dataset (GISTEMP Team , 2023).

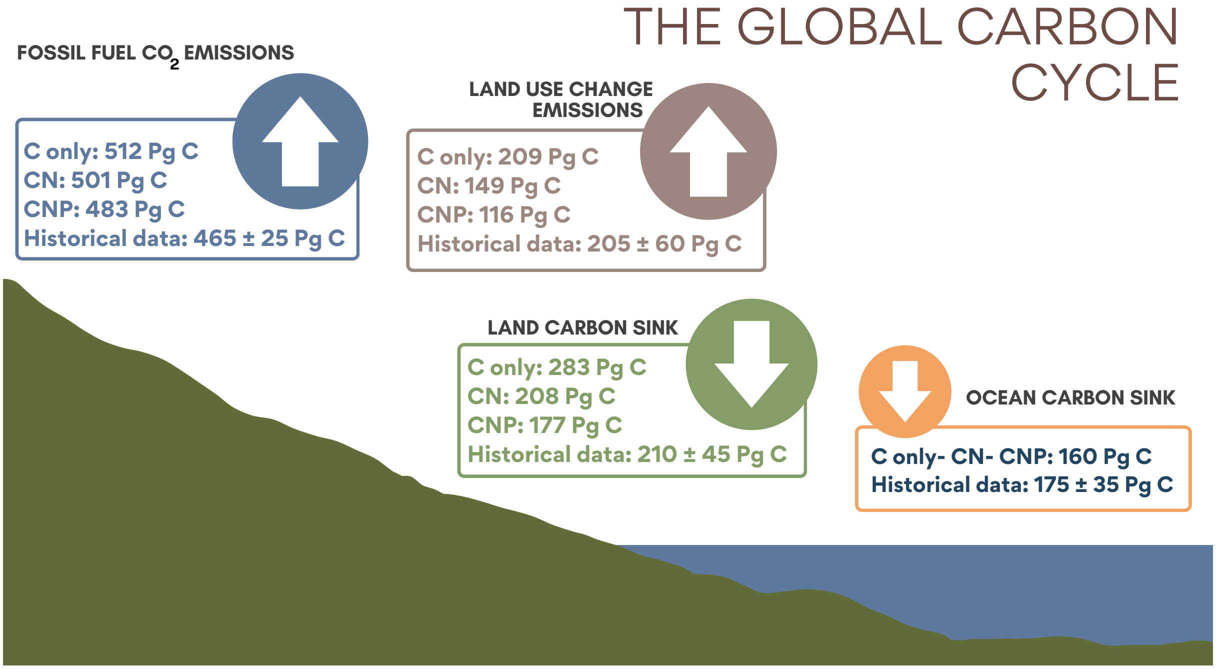

Figure 2. Historical 1850-2021 cumulative land carbon sink, ocean sink, land use change emissions and diagnosed CO_2 emissions simulated compared to Friedlingstein et al. (2022).

3.3 Zero Emission Commitment

To analyse the impact of nutrient limitation in zero emission scenarios, ZECMIP type experiments were conducted in C-only, CN and CNP. Figure 3 show the temperature anomaly relative to the estimated temperature at the year of cessation. The temperature pattern in the 100 years following cessation is similar for all the model structures. There is an initial rise of temperature around the 20th year and a quick decline on the 35-40th year, followed by an increase around the 70-80th year. A difference between C-only and CN and CNP is that the C-only simulation increase is lower than the nutrient limited simulations.The overall ZEC value is higher in CNP and CN than in C-only. Higher ZEC values indicate a larger increase of temperature after emissions have ceased. For CN and CNP the ZEC_{50} value resulted in 0.07 and 0.09 °C compared to 0.02 °C in C-only. These values are similar to the ZEC_{50} of 0.03 °C shown in MacDougall et al. (2020) for the same model. The ZEC across 100 years of simulation after emission have ceased show a larger difference in temperature change after emission have ceased. C-only resulted in 0.05 °C compared to 0.17 °C in CN and 0.21 °C in CNP. This represent a relevant increase of temperature after emission have ceased in the nutrient limited simulations.

3.4 Estimated contribution of non-CO_2 climate forcing to future warming

In this section we assessed the remaining carbon budgets variability between different nutrient limitation model structures in the eight SSPs used in CMIP6. Furthermore, our emphasis was to show the role of N and P representation in remaining carbon budgets estimates from different future scenarios. Figures 4-8 show the resulting remaining carbon budgets for SSP 1-1.9, 1-2.6, 2-4.5, 3-7.0, 4-3.4, 4-6.0, 5-3.4 and 5-8.5. Given the different SSPs forcing and resulting warming, not all experimental simulations crossed the 2, 2.5 and 3 °C thresholds.. SSP1-1.9 and SSP1-2.6 only reached the 1.5 °C target, SSP 4-3.4 and SSP 5-3.4 only reached the 2 °C target, SSP 2-4.5 reached the 2.5 °C target and SSP 3-7.0, SSP 4-6.0 and SSP 5-8.5 reached the 3 °C target. The remaining carbon budgets estimates and the SSP temperatures anomalies can be seen in more detailed in Appendix A1, A2, A3 and B1. Overall, the application of nutrient limitation increased the TCRE and hence, decrease the carbon budget for all set targets. As expected, among CN and CNP simulation phosphorus limitation reduced the remaining carbon budgets. The mean remaining carbon budgets estimated among the SSPs simulations for ECS 3.4 [ECS 4.5 to ECS 2] in the C-only, CN and CNP for 1.5 °C target were: 228[31 to 291], 185[25 to 259] and 175[9 to 223] Pg C respectively. For the 2 °C target the mean remaining carbon budget were 471[205 to 554], 373[154 to 479] and 351[137 to 402] Pg C for the C, CN and CNP configurations respectively. The remaining carbon budgets for the 2.5 °C target were 719[378 to 869], 591[321 to 725] and 596[315 to 673] Pg C. Finally, the remaining carbon budgets for the 3 °C target were 974.4[546 to 1174], 798[460 to 986] and 796[467 to 920] Pg C. This represents a reduction of 19 and 24 % for the 1.5 °C target, 21 and 26 % for the 2 °C target, 18 and 17% for the 2.5 °C target and finally 18 and 19 % for the 3 °C target in CN and CNP compared to C-only.

One of the impacts of nutrient limitation is in the change of land use change emissions corresponding to the reduction and change of vegetation. We found that the mean land use change emission budget among SSPs simulation from year 2020 to the 1.5 °C target in the ECS 3.4[ECS 4.5 to ECS 2] were: 31[2 to 39], 20[2 to 40] and 13[1 to 23] Pg C for C-only, CN and CNP respectively (Figure 9). Corresponding to a reduction of 11.2 and 18.4 Pg C in CN and CNP compared to C-only. These

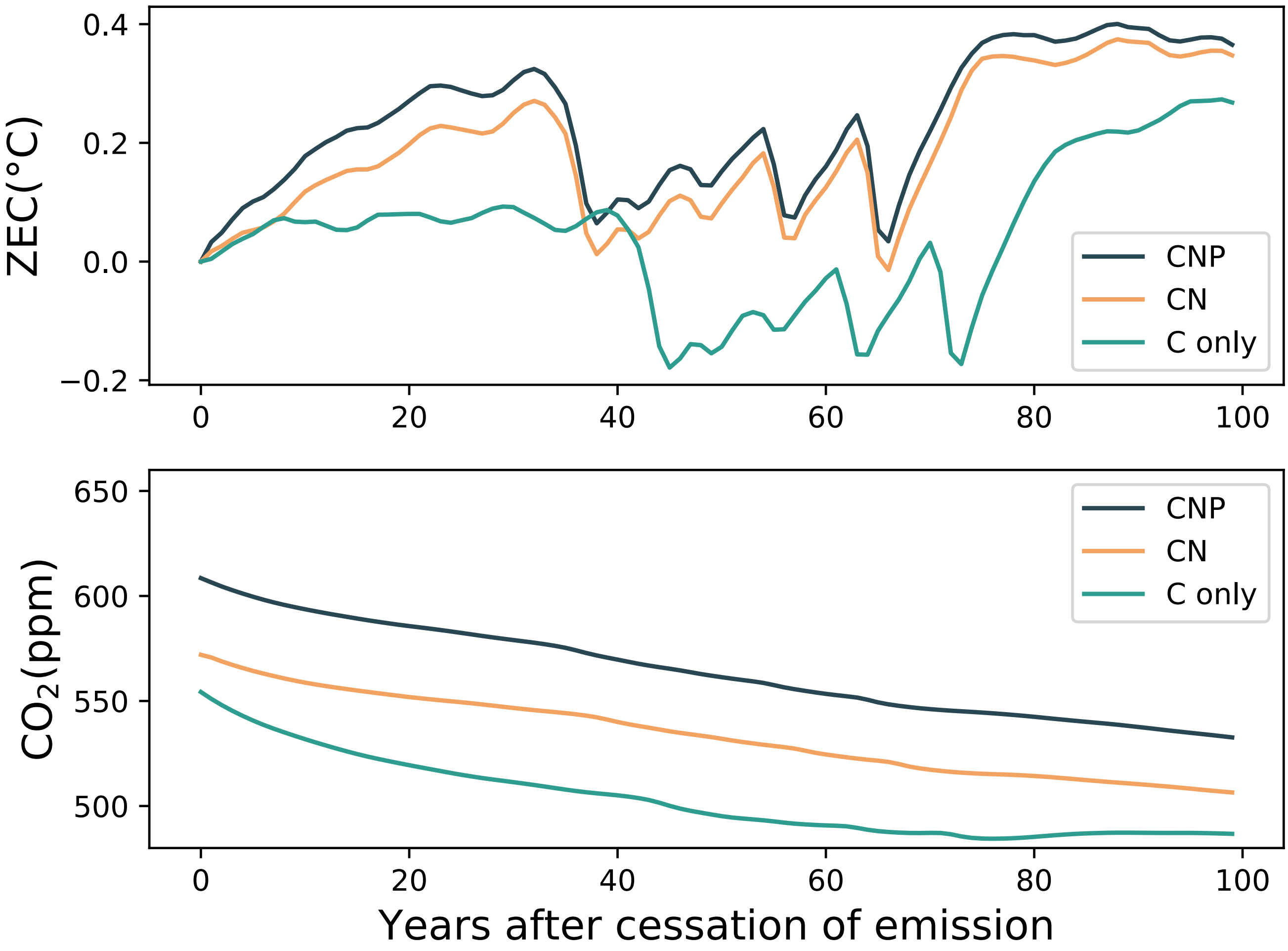

Figure 3. Zero Emissions Commitment following the cessation of emissions during the experiment wherein 1000 PgC was emitted following the 1pctCO2 experiment. ZEC is the temperature anomaly relative to the estimated temperature at the year of cessasion. Note the UVic ESCM lacks internal variability. The rapid changes in global temperature seen in the top panel are due to disruptions to the ocean meridional overturing circulation (Mengis et al. , 2020)

results demonstrate that the remaining carbon budget is clearly sensitive to the availability of nutrients represented in SSPs model simulations. As shown in figure 2-8 the remaining carbon budgets vary between the SSPs scenarios as temperature rise are effected by non-CO_2 forcings, corresponding to socioeconomical global uncertainties. Furthermore, the land carbon cycle in this case nutrient limitation, represents an implicit uncertainty under these different socioeconomical projections.

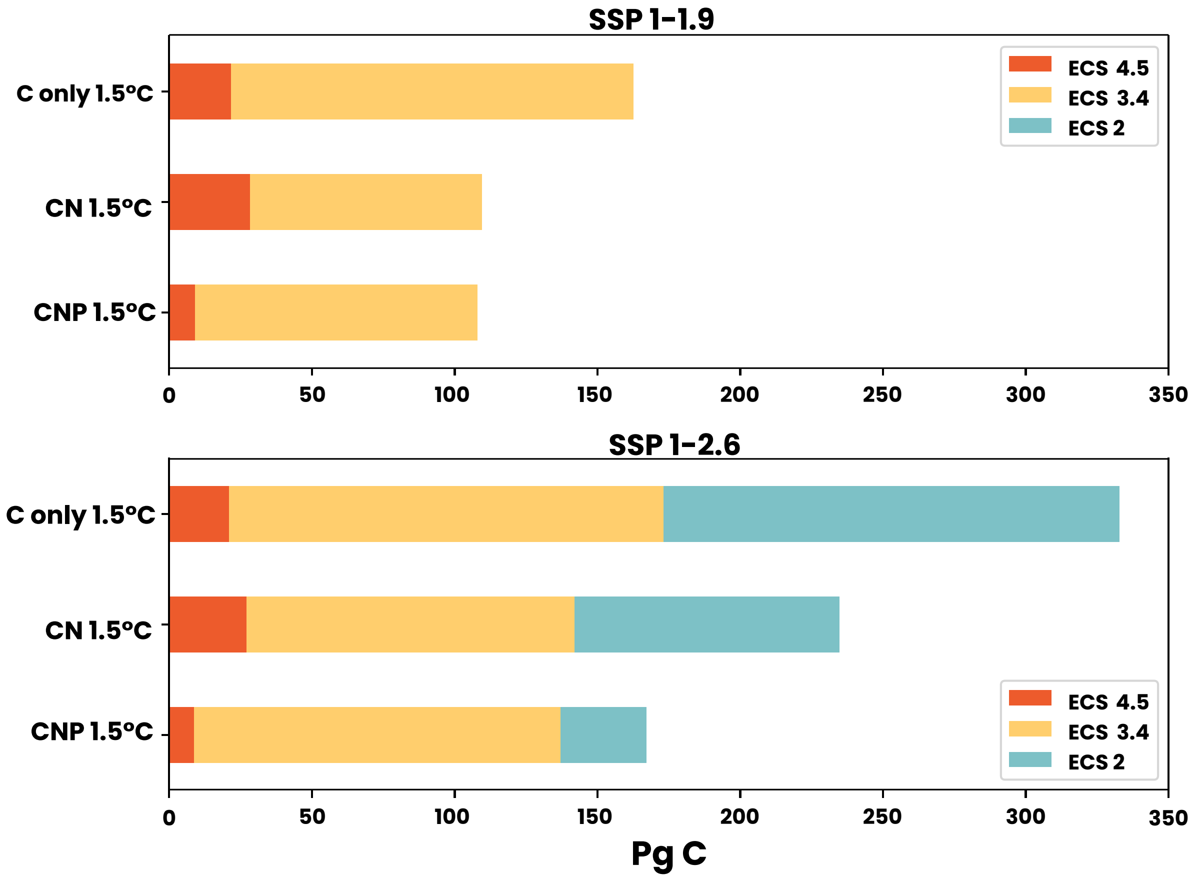

Figure 4. Carbon budgets for the 1.5 °C target for SSP 1-1.9 and 1-2.6. Three model sensitivities are shown as: ECS 4.5 orange, ECS 3.4 yellow and ECS 2 blue.

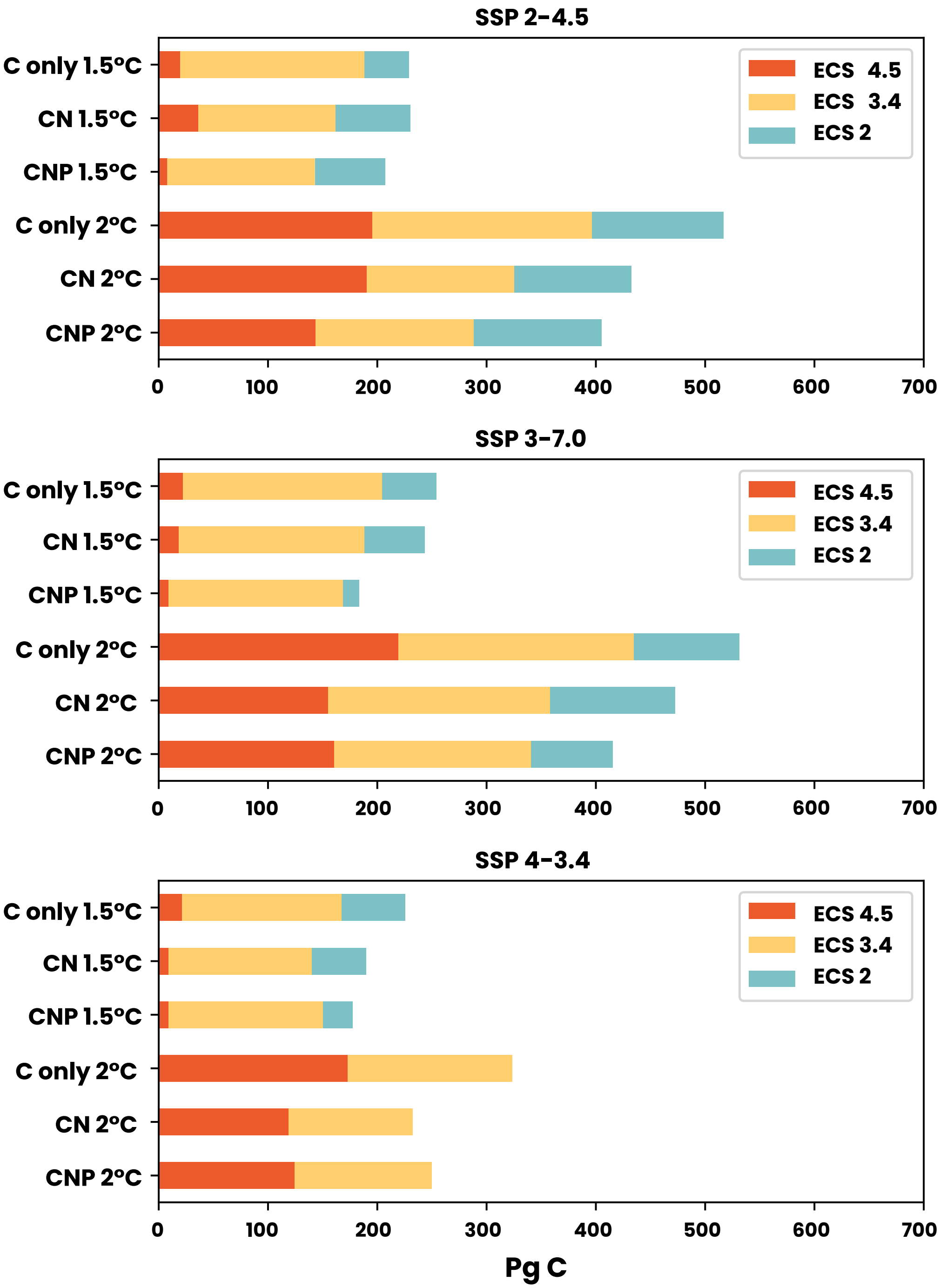

Figure 5. Carbon budgets for the 1.5 and 2 °C targets for SSP 2-4.5, 3-7.0 and 4-3.4. Three model sensitivities are shown as: ECS 4.5 orange, ECS 3.4 yellow and ECS 2 blue.

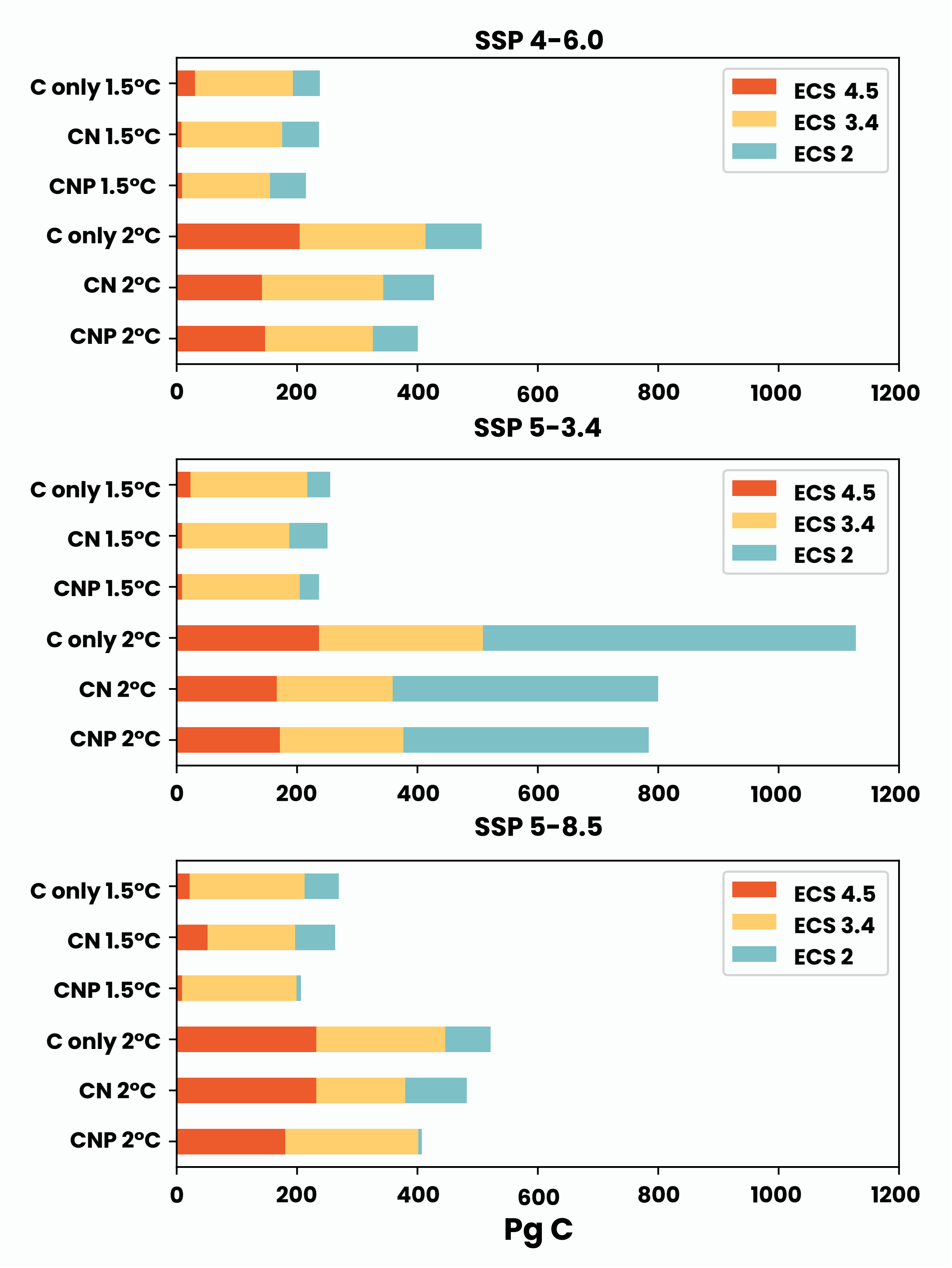

Figure 6. Carbon budgets for the 1.5 and 2 °C targets for SSP 4-6.0, 5-3.4 and 5-8.5. Three model sensitivities are shown as: ECS 4.5 orange, ECS 3.4 yellow and ECS 2 blue.

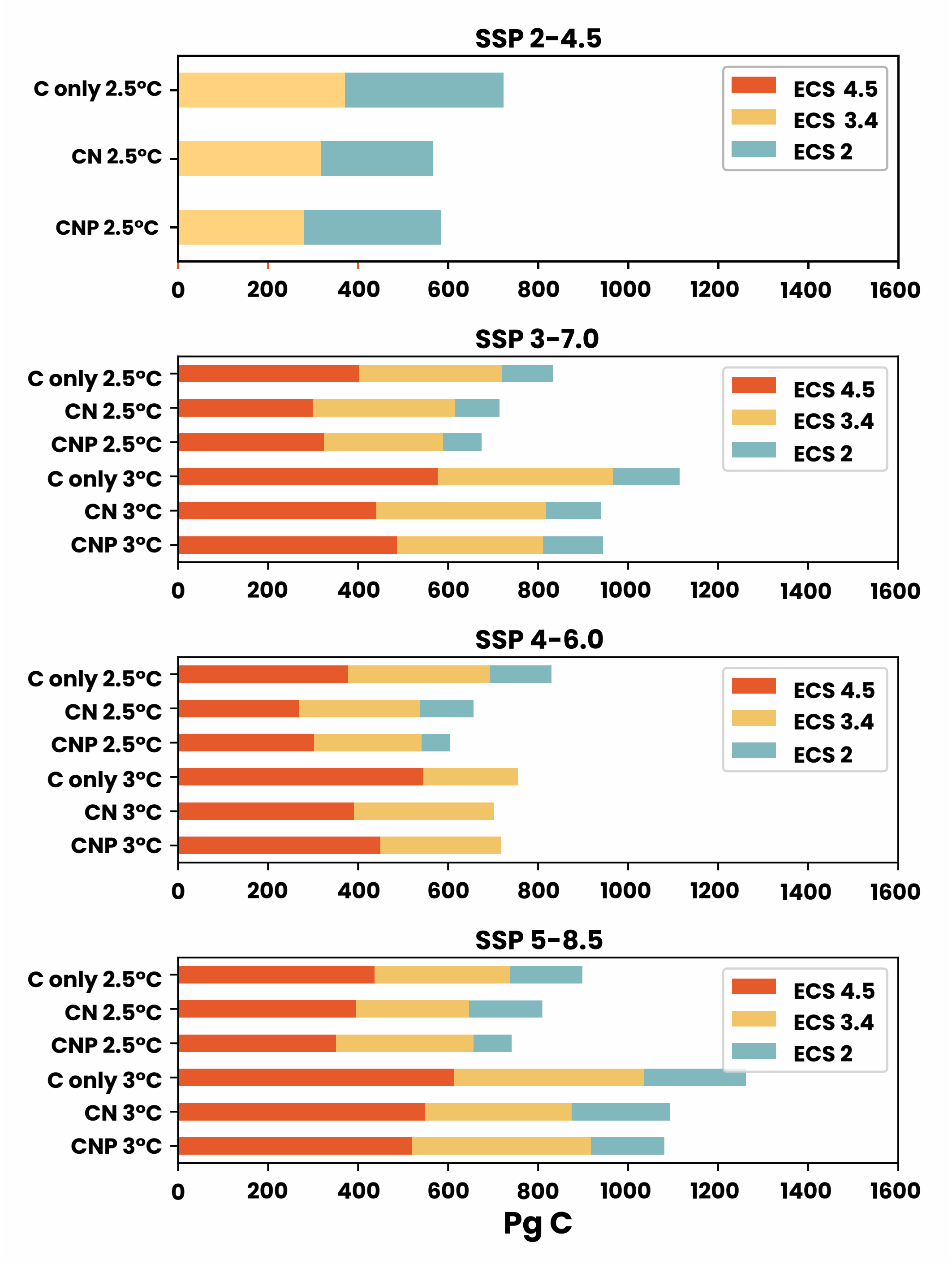

Figure 7. Carbon budgets for the 2.5, 3 °C targets for SSP 3-7.0, 4-6.0 and 5-8.5. These were the only scenarios that reached the threshold. Three model sensitivities are shown as: ECS 4.5 orange, ECS 3.4 yellow and ECS 2 blue.

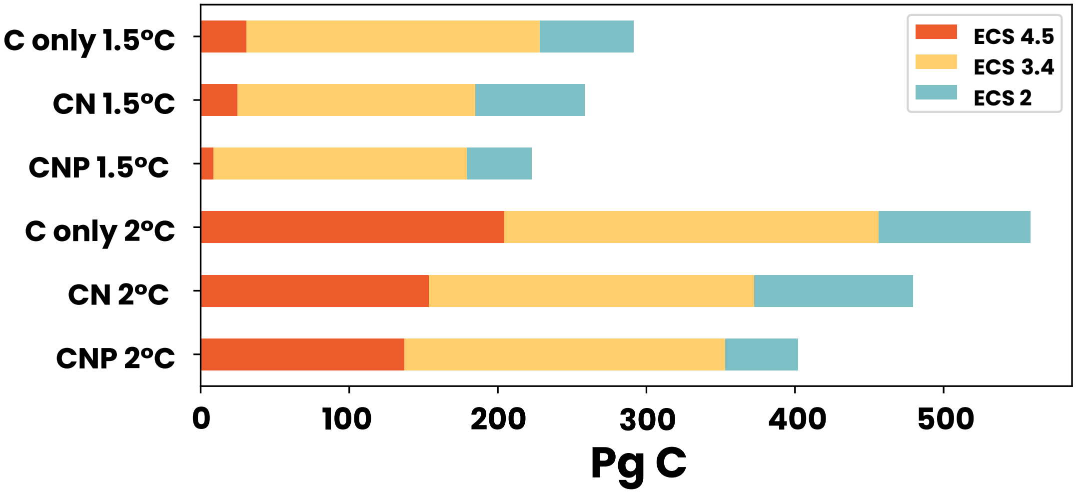

Figure 8. Mean SSP carbon budgets for the 1.5 and 2 °C temperature targets.

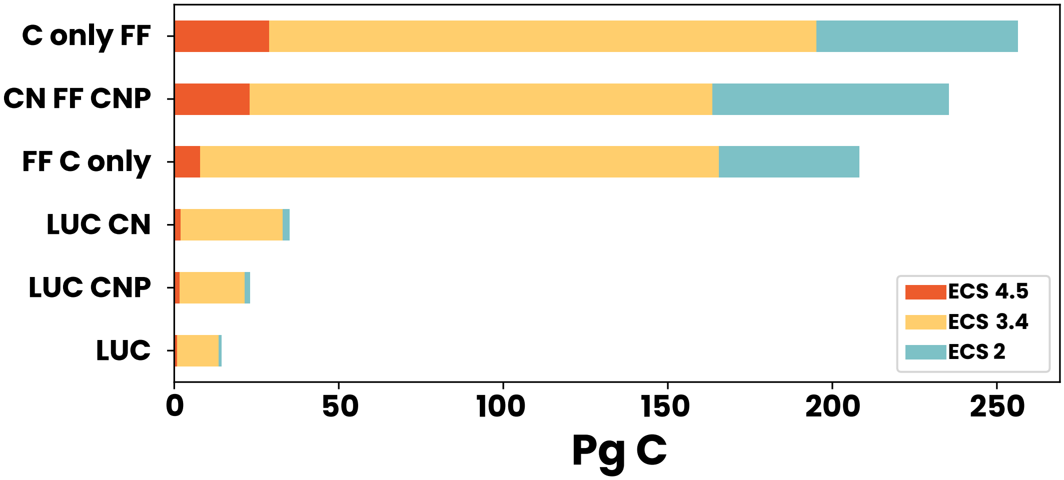

Figure 9. Mean SSP carbon budgets for Fossil Fuel (FF) and LUC emissions for the 1.5 °C temperature target.

4 Discussion

The representation of the carbon cycle in Earth system models has been shown to be a source of uncertainty in the estimation of remaining carbon budgets (Matthews et al. , 2020). In nutrient-limited structures, the capacity of land to uptake atmospheric carbon is a constrainted (Wang et al. , 2010; Wieder et al. , 2015; Wang and Goll , 2021; Wei et al. , 2022; De Sisto et al. , 2023). This study shows a decrease in land carbon sink in nutrient-limited simulations, agreeing with other nutrient-limited model structures in literature (Wang et al. , 2010; Wieder et al. , 2015; Wang and Goll , 2021). In contrast, the reduced carbon uptake by plants is balanced by a decreased of land use change emissions. This reduction comes in the UVic ESCM due to a decrease of vegetation biomass, especially from woody plants (De Sisto et al. , 2023). This is also shown in Wang et al. (2015), where the implementation of nutrient-limited models reduced the carbon emissions from deforestation in RCP8.5 scenarios.

The reduction of vegetation biomass also leads to an increase of albedo due to the replacement of broadleaf trees and needleaf trees with grass or bare soil, as shown in (De Sisto et al. , 2023). The albedo differences among nutrient-model structures have a marginal effect on temperature. It is interesting to note that in nature, there are observations pointing to positive correlations between the concentration of nitrogen in canopies and albedo (Loozen et al. , 2020). This correlation is not reflected in the model structure as high nitrogen concentrations would reduce the leaf "shed" when the model is considered to be under nutrient limitation.

The change of terrestrial carbon fluxes under nutrient limitation is shown in this study to accelerate warming, impacting the time when temperature thresholds are reached in different simulations. Hence, corresponding to an increase of the TCRE. In concentration driven simulations the diagnosed cumulative emissions estimated by the model under nutrient limitation is lower than C-only simulations, as in figure 2. The main reason being the decrease of land carbon flux. The carbon sink in terrestrial systems was noted as one of the most significant sources of uncertainties in TCRE estimated (Jones and Friedlingstein , 2020). Other unrepresented terrestrial processes, such as permafrost thawing, have also been shown to affect the TCRE and remaining carbon budgets (MacDougall et al. , 2015).

After cessation of emissions, the terrestrial nutrient limitation was shown to increase the temperature response after emissions have ceased. The ZEC values are within the range of values of -0.36 to 0.29 °C presented by MacDougall et al. (2020) who analysed model simulations from 9 ESMs and 9 Earth system model of intermediate complexity. The land carbon sink has been identified as a critical process in ZEC values (MacDougall et al. , 2020; Palazzo et al. , 2023). After emissions ceased the reduced rate of carbon sink by terrestrial systems increases the immediate temperature response of the systems in nutrient limited simulations. This decreased sink, leads to an overall reduction of ZEC compared to C-only simulations.

In this study, the effect of terrestrial nutrient limitation on the terrestrial carbon dynamics resulted in the reduction of the remaining carbon budgets, decreasing the allowable emissions by 19% to 25% in the 1.5 and 2 °C targets. This substantial amount is why terrestrial N and P limitation should be considered in the estimation of remaining carbon budgets. The IPCC AR6 (IPCC 2021) reports remaining carbon budgets estimates from 2020 of 245, 177, 136, 108 and 82 PgC for the 1.5 °C target with a probability of 17, 33, 50, 67 and 83% respectively. Compared to the 50% of probability of 136 PgC our nutrient-limited model simulations, CN 185 PgC and CNP 175 PgC estimated a closer value than the C-only 228 PgC. Hence, nutrient-limited simulations estimates from the UVic ESCM closer to the multi-model mean.

As unrepresented processes in other models, N and P limitation reduced the estimated remaining carbon budget in CN and CNP by 43 and 53 PgC for the 1.5 °C target and 98 and 120 PgC for the 2 °C target when compared to the C-only simulation. These estimations are larger than the roughly estimate of 27 PgC reduction of carbon budgets due to unrepresented carbon feedbacks (Rogelj et al. , 2018), suggesting that this value may have been underestimated in the IPCC 1.5°C report.

Regarding the uncertainties in the terrestrial nitrogen and phosphorus cycles, the main limitation of terrestrial N and P cycles is the lack of global observational data that can be used to refine and validate ESMs. The lack of data includes most of the N and P cycle processes. Other uncertainties on the representation of terrestrial nutrient limitation in the UVic ESCM include the lack of a dynamic leaf nutrient resorption representation, lack of root uptake constraints, simplified sorption-resorption dynamics of phosphorus in soils, and a simplified wetland representation. A detailed description of the terrestrial N and P uncertainties can be found in the complete description of the model in (De Sisto et al. , 2023).

5 Conclusion

Remaining carbon budgets are crucial for climate policy and management. As the remaining carbon budgets is intrinsically linked to the TCRE and the dynamics of the global carbon budget, it is important to consider the uncertainties that nutrient limitation has on our terrestrial model structures. In this study we found that nutrient limitation, in this case N and P had a considerable effect on the remaining carbon budgets estimates. Historically, N and P limitation reduced the land carbon sink and land use change emission. The range of reduction of land carbon sink was: 75 to 106 Pg C and the range of reduction for the land use change emission was: 60 to 93 Pg C. Overall under the Shared Socioeconomic Pathways, N and P reduced the remaining carbon budgets estimates for 1.5, 2, 2.5 and 3 °C targets. CN and CNP showed a reduction of 43 and 53 Pg C for the 1.5 °C target and 98 and 120 Pg C for the 2 °C target respectively when compared to C-only. Theses values represent a reduction of 19 and 24 % for the 1.5 °C target, 21 and 26 % for the 2 °C target. After emission have ceased N and P had a relevant impact on the temperature change, the ZEC across 100 years of simulations after emission have ceased showed an increase in temperature for the nutrient limited simulations CN and CNP of 0.12 and 0.16 °C when compared to C-only. The uncertainty of the magnitude of the reduction in the remaining carbon budget from nutrient limitation will be more clear if a multimodel assessment is conducted. Overall we assess that accounting for nutrient limitations will lead to a substantial reduction in the estimated remaining carbon budget.

Appendix A

Table A1. Remaining carbon budgets from the Shared Socioeconomic Pathways: SSP 2- 4.5, 3- 7.0 and 4- 3.4 simulations for 1.5, 2°C targets relative to a warming from 1850-1900.

SSP scenarios	Target	Climate sensitivity	C-only(PgC)	CN(PgC)	CNP(PgC)
1- 1.9	1.5 °C	4.5	20	22	8
1- 1.9	1.5 °C	3.4	163	110	108
1- 1.9	1.5 °C	2	Not reached	Not reached	Not reached
1- 2.6	1.5 °C	4.5	21	27	9
1- 2.6	1.5 °C	3.4	173	142	137
1- 2.6	1.5 °C	2	332	235	167
2- 4.5	1.5 °C	4.5	21	37	9
2- 4.5	1.5 °C	3.4	189	161	144
2- 4.5	1.5 °C	2	231	231	208
2- 4.5	2 °C	4.5	197	191	144
2- 4.5	2 °C	3.4	397	325	288
2- 4.5	2 °C	2	516	433	406
3- 7.0	1.5 °C	4.5	23	19	9
3- 7.0	1.5 °C	3.4	204	189	170
3- 7.0	1.5 °C	2	255	244	184
3- 7.0	2 °C	4.5	220	155	161
3- 7.0	2 °C	3.4	435	359	343
3- 7.0	2 °C	2	532	473	416
4- 3.4	1.5 °C	4.5	22	9	- 9
4- 3.4	1.5 °C	3.4	168	141	150
4- 3.4	1.5 °C	2	226	190	178
4- 3.4	2 °C	4.5	174	119	125
4- 3.4	2 °C	3.4	324	233	250
4- 3.4	2 °C	2	Not reached	Not reached	Not reached

Table A2. Remaining carbon budgets from the Shared Socioeconomic Pathways simulations: SSP 4- 6.0, 5- 3.4 and 5- 8.5 for 1.5, 2°C targets relative to a warming from 1850-1900.

SSP scenarios	Target	Climate sensitivity	C-only(PgC)	CN(PgC)	CNP(PgC)
4- 6.0	1.5 °C	4.5	32	8	10
4- 6.0	1.5 °C	3.4	194	177	157
4- 6.0	1.5 °C	2	238	236	215
4- 6.0	2 °C	4.5	174	119	125
4- 6.0	2 °C	3.4	324	233	250
4- 6.0	2 °C	2	Not reached	Not reached	Not reached
5- 3.4	1.5 °C	4.5	25	12	10
5- 3.4	1.5 °C	3.4	219	189	204
5- 3.4	1.5 °C	2	255	251	236
5- 3.4	2 °C	4.5	238	169	174
5- 3.4	2 °C	3.4	509	359	378
5- 3.4	2 °C	2	1129	800	785
5- 8.5	1.5 °C	4.5	22	52	12
5- 8.5	1.5 °C	3.4	211	199	198
5- 8.5	1.5 °C	2	270	264	210
5- 8.5	2 °C	4.5	233	232	183
5- 8.5	2 °C	3.4	446	380	403
5- 8.5	2 °C	2	570	504	446

Table A3. Remaining carbon budgets from the Shared Socioeconomic Pathways simulations: SSP-2.45, SSP 3-7.0, 4-6.0 and 5-8.5 for 2.5, 3°C targets relative to a warming from 1850-1900.

SSP scenarios	Target	Climate sensitivity	C-only(PgC)	CN(PgC)	CNP(PgC)
2- 4.5	2.5 °C	4.5	373	321	282
2- 4.5	2.5 °C	3.4	721	567	584
2- 4.5	2.5 °C	2	Not reached	Not reached	Not reached
3- 7.0	2.5 °C	4.5	405	303	325
3- 7.0	2.5 °C	3.4	722	616	591
3- 7.0	2.5 °C	2	830	714	676
3- 7.0	3 °C	4.5	580	444	490
3- 7.0	3 °C	3.4	967	820	816
3- 7.0	3 °C	2	1118	939	942
4- 6.0	2.5 °C	4.5	380	271	303
4- 6.0	2.5 °C	3.4	670	528	542
4- 6.0	2.5 °C	2	830	658	601
4- 6.0	3 °C	4.5	545	391	454
4- 6.0	3 °C	3.4	756	703	717
4- 6.0	3 °C	2	Not reached	Not reached	Not reached
5- 8.5	2.5 °C	3.4	437	398	356
5- 8.5	2.5 °C	3.4	742	648	658
5- 8.5	2.5 °C	2	900	809	742
5- 8.5	3 °C	4.5	615	552	521
5- 8.5	3 °C	3.4	1037	875	918
5- 8.5	3 °C	2	1260	1093	1080

Appendix B: Temperature anomalies of the SSP simulations for C-only, CN and CNP

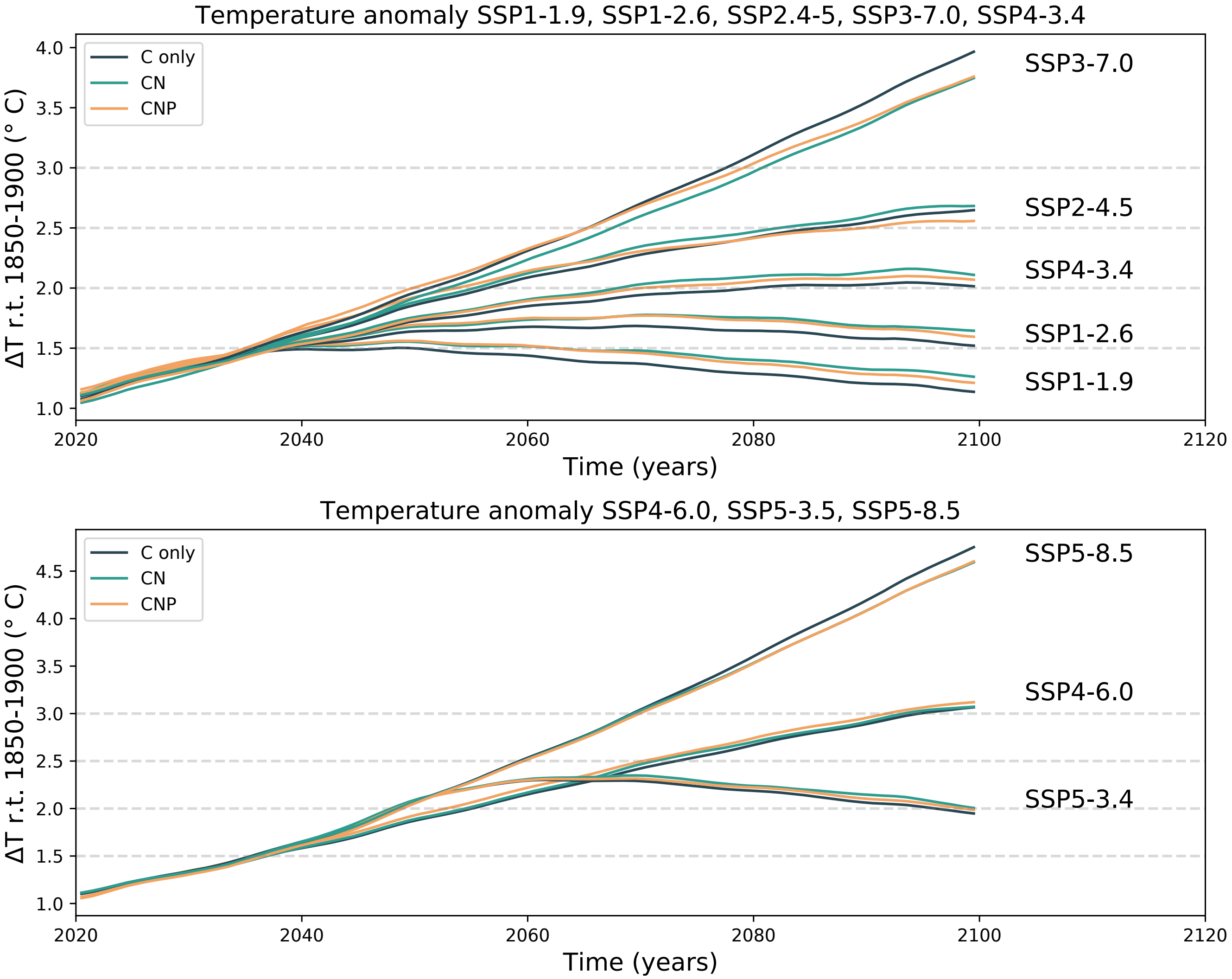

Figure B1. SSP temperature anomaly relative to 1850-1900 of C-only, CN and CNP simulations.

Code and data availability.

The current version of the model is available from the project website: http://terra.seos.uvic.ca/model/2.10/. The exact version of the model used to produce the results used in this paper is archived on:
https://borealisdata.ca/dataset.xhtml?persistentId=doi:10.5683/SP3/GXYZKU (De Sisto , 2022).

Author contributions.

MD conducted model simulations and data analysis. MD wrote the paper and AHMD provided supervisory support.

Competing interests.

The authors declare that they have no conflict of interest.

Acknowledgements. AHMD and MD are grateful for support from the Natural Science and Engineering Research Council of Canada Discovery Grant program and support from Compute Canada (now the Digital Research Alliance of Canada).

References

Achat, D., Gallet-Budynek, A. and Loustau, D: Future challenges in coupled C–N–P cycle models for terrestrial ecosystems under global change: a review. Biogeochemistry, 131, 10.1007/s10533-016-0274-9, 2016.

Archer, D.: A data-driven model of the global calcite lysocline, Global Biogeochem. Cy., 10, 511–526, https://doi.org/10.1029/96GB01521, 1996.

Arias, P.A., Bellouin, N., Coppola, E., Jones, R.G., Krinner, G., Marotzke, J., Naik, V., Palmer, M.D., Plattner, G.-K., Rogelj, J., Rojas, M., Sillmann, J., Storelvmo, T., Thorne, P.W., Trewin, B., Achuta Rao, K., Adhikary, B., Allan, R.P., Armour, K., Bala, G., Barimalala, R., Berger, S., Canadell, J.G., Cassou, C., Cherchi, A., Collins, W., Collins, W.D., Connors, S.L., Corti, S., Cruz, F., Dentener, F.J., Dereczynski, C., Di Luca, A., Diongue Niang, A., Doblas-Reyes, F.J., Dosio, A., Douville, H., Engelbrecht, F., Eyring, V., Fischer, E., Forster, P., Fox-Kemper, B., Fuglestvedt, J.S., Fyfe, J.C., Gillett, N.P., Goldfarb, L., Gorodetskaya, I., Gutierrez, J.M., Hamdi, R., Hawkins, E., Hewitt, H.T., Hope, P., Islam, A.S., Jones, C., Kaufman, D.S., Kopp, R.E., Kosaka, Y., Kossin, J., Krakovska, S., Lee, J.-Y., Li, J., Mauritsen, T., Maycock, T.K., Meinshausen, M., Min, S.-K., Monteiro, P.M.S., Ngo-Duc, T., Otto, F., Pinto, I., Pirani, A., Raghavan, K., Ranasinghe, R., Ruane, A.C., Ruiz, L., Sallée, J.-B., Samset, B.H., Sathyendranath, S., Seneviratne, S.I., Sörensson, A.A., Szopa, S., Takayabu, I., Tréguier, A.-M., van den Hurk, B., Vautard, R., von Schuckmann, K., Zaehle, S., Zhang, X., and Zickfeld, K: Technical Summary. In Climate Change 2021: The Physical Science Basis. Contribution of Working Group I to the Sixth Assessment Report of the Intergovernmental Panel on Climate Change [Masson-Delmotte, V., Zhai, P., Pirani, A., Connors, S.L., Péan, C., Berger, S., Caud, N., Chen, Y., Goldfarb, L., Gomis, M.I., Huang, M., Leitzell, K., Lonnoy, E., Matthews, J.B.R., Maycock, T.K., Waterfield, T., Yelekçi, O., Yu, R., and Zhou, B. (Eds.)]. Cambridge University Press, Cambridge, United Kingdom and New York, NY, USA, pp. 33-144. doi:10.1017/9781009157896.002, 2021.

Arora, V. K., Katavouta, A., Williams, R. G., Jones, C. D., Brovkin, V., Friedlingstein, P., Schwinger, J., Bopp, L., Boucher, O., Cadule, P., Chamberlain, M. A., Christian, J. R., Delire, C., Fisher, R. A., Hajima, T., Ilyina, T., Joetzjer, E., Kawamiya, M., Koven, C. D., Krasting, J. P., Law, R. M., Lawrence, D. M., Lenton, A., Lindsay, K., Pongratz, J., Raddatz, T., Séférian, R., Tachiiri, K., Tjiputra, J. F., Wiltshire, A., Wu, T., and Ziehn, T.: Carbon–concentration and carbon–climate feedbacks in CMIP6 models and their comparison to CMIP5 models, Biogeosciences, 17, 4173–4222, https://doi.org/10.5194/bg-17-4173-2020, 2020.

Avis, C. A.: Simulating the Present-Day and Future Distribution of Permafrost in the UVic Earth System Climate Model, PhD thesis, University of Victoria, 2012.

Bauer, N., Calvin, K., Emmerling, J., Fricko, O., Fujimori, S., Hilaire, J., Eom, J., Krey, V., Kriegler, E., Mouratiadou, I., de Boer, H.S., van den Berg, M., Carrara, S., Daioglou, V., Drouet, L., Edmonds, J.E., Gernaat, D., Havlik, P., Johnson, N., Klein, D., Kyle, P., Marangoni, G., Masui, T., Pietzcker, R.C., Strubegger, M., Wise, M., Riahi, K., and van Vuuren, D.P: Shared Socio-Economic Pathways of the Energy Sector – Quantifying the Narratives. Global Environmental Change, 42, 316-330, https://doi.org/10.1016/j.gloenvcha.2016.07.006, 2017.

Bitz, C. M., Holland, M. M., Weaver, A. J., and Eby, M.: Simulating the ice-thickness distribution in a coupled, J. Geophys. Res., 106, 2441–2463, https://doi.org/10.1029/1999JC000113, 2001.

Bodirsky, B.L., Rolinski, S., Biewald, A., Weindl, I., Popp, A., et al: Global Food Demand Scenarios for the 21st Century, PLOS ONE, 10(11), e0139201, https://doi.org/10.1371/journal.pone.0139201, 2015.

Bonan, G. B. and Levis, S.: Quantifying carbon-nitrogen feedbacks in the Community Land Model (CLM4), Geophys. Res. Lett., 37, 2261–2282, 2010.

Cox, P. M., Betts, R. A., Bunton, C. B., Essery, R. L. H., Rowntree, P. R., and Smith, J.: The impact of new land surface physics on the GCM simulation of climate and climate sensitivity, Clim. Dynam., 15, 183–203, 1999.

Cox, P. M.: Description of the TRIFFID dynamic global vegetation model, Tech. Rep. 24, Hadley Centre, Met office, London Road, Bracknell, Berks, RG122SY, UK, 2001.

De Sisto, M. L., MacDougall, A. H., Mengis, N., and Antoniello, S.: Modelling the terrestrial nitrogen and phosphorus cycle in the UVic ESCM, Geosci. Model Dev., 16, 4113–4136, https://doi.org/10.5194/gmd-16-4113-2023, 2023.

De Sisto, M: Modelling the terrestrial nitrogen and phosphorus cycle in the UVic ESCM, https://doi.org/10.5683/SP3/GXYZKU, Borealis, V1, 2022.

Du, E., Terrer, C., Pellegrini, A., Ahlstrom, A., Van Lissa, C., Zhao, X., Xia, N., Wu, X. and Jackson, R.: Global patterns of terrestrial nitrogen and phosphorus limitation, Nat. Geosci. 13, 221–226, https://doi.org/10.1038/s41561-019-0530-4, 2020.

Eby, M., Weaver, A. J., Alexander, K., Zickfeld, K., Abe-Ouchi, A., Cimatoribus, A. A., Crespin, E., Drijfhout, S. S., Edwards, N. R., Eliseev, A. V., Feulner, G., Fichefet, T., Forest, C. E., Goosse, H., Holden, P. B., Joos, F., Kawamiya, M., Kicklighter, D., Kienert, H., Matsumoto, K., Mokhov, I. I., Monier, E., Olsen, S. M., Pedersen, J. O. P., Perrette, M., Philippon-Berthier, G., Ridgwell, A., Schlosser, A., Schneider von Deimling, T., Shaffer, G., Smith, R. S., Spahni, R., Sokolov, A. P., Steinacher, M., Tachiiri, K., Tokos, K., Yoshimori, M., Zeng, N., and Zhao, F.: Historical and idealized climate model experiments: an intercomparison of Earth system models of intermediate complexity, Clim. Past, 9, 1111–1140, https://doi.org/10.5194/cp-9-1111-2013, 2013.

Eyring, V., Bony, S., Meehl, G. A., Senior, C. A., Stevens, B., Stouffer, R. J., and Taylor, K. E.: Overview of the Coupled Model Intercomparison Project Phase 6 (CMIP6) experimental design and organization, Geosci. Model Dev., 9, 1937–1958, https://doi.org/10.5194/gmd-9-1937-2016, 2016.

Fanning, A. F., and Weaver, A. J.: An atmospheric energy-moisture balance model: Climatology, interpentadal climate change, and coupling to an ocean general circulation model, Journal of Geophysical Research, 101, 15111, 1996.

Filippelli, G.: The global phosphorus cycle, in phosphates: Geochemical, geobiological, and materials importance, Reviews in Mineralogy and Geochemistry, 391-425. 2002.

Fisher, J., Badgley, G. and Blyth, E.: Global nutrient limitation in terrestrial vegetation, Global Biogeochemical Cycles 6, https://doi.org/10.1029/2011GB004252, 2012.

Fowler, D., Coyle, M., Skiba, U., Sutton, M. A., Cape, J. N., Reis, S., Sheppard, L. J., Jenkins, A., Grizzetti, B., Galloway, J. N., Vitousek, P., Leach, A., Bouwman, A. F., Butterbach-Bahl, K., Dentener, F., Stevenson, D., Amann, M., and Voss, M.: The global nitrogen cycle in the twenty-first century, Philosophical transactions of the Royal Society of London. Series B, Biological sciences, 368(1621), https://doi.org/10.1098/rstb.2013.0164, 2013.

Friedlingstein, P., Jones, M. W., O'Sullivan, M., Andrew, R. M., Bakker, D. C. E., et al.: Global Carbon Budget 2021, Earth Syst. Sci. Data, 14, 1917–2005, https://doi.org/10.5194/essd-14-1917-2022, 2022.

GISTEMP Team, 2023: GISS Surface Temperature Analysis (GISTEMP), version 4. NASA Goddard Institute for Space Studies. Dataset accessed 2023-01-02 at https://data.giss.nasa.gov/gistemp/.

Goll, D., Brovkin, V., Parida, B., Reick, C., Kattge, J., Reich, P., van Bodegom, P., and Niinemets, Ü.: Nutrient limitation reduces land carbon uptake in simulations with a model of combined carbon, nitrogen and phosphorus cycling, Biogeosciences 9, 3547–3569, https://doi.org/10.5194/bg-9-3547-2012, 2012.

Goll, D., Vuichard, N., Maignan, F., Jornet-Puig, A., Sardans, J., Violette, A., Peng, S., Sun, Y., Kvakic, M., Guimberteau, M., Guenet, B., Zaehle, S., Penuelas, J., Janssens, I. and Ciais, P.: A representation of the phosphorus cycle for ORCHIDEE. Geoscientific Model Development 10, 3745-3770, doi.org/10.5194/gmd-10-3745-2017, 2017.

IPCC, 2021: Summary for Policymakers. In: Climate Change 2021: The Physical Science Basis. Contribution of Working Group I to the Sixth Assessment Report of the Intergovernmental Panel on Climate Change [Masson-Delmotte, V., P. Zhai, A. Pirani, S.L. Connors, C. Péan, S. Berger, N. Caud, Y. Chen, L. Goldfarb, M.I. Gomis, M. Huang, K. Leitzell, E. Lonnoy, J.B.R. Matthews, T.K. Maycock, T. Waterfield, O. Yelekçi, R. Yu, and B. Zhou (eds.)]. In Press.

Jones, C. D., Frölicher, T. L., Koven, C., MacDougall, A. H., Matthews, H. D., Zickfeld, K., Rogelj, J., Tokarska, K. B., Gillett, N. P., Ilyina, T., Meinshausen, M., Mengis, N., Séférian, R., Eby, M., and Burger, F. A.: The Zero Emissions Commitment Model Intercomparison Project (ZECMIP) contribution to C4MIP: quantifying committed climate changes following zero carbon emissions, Geosci. Model Dev., 12, 4375–4385, https://doi.org/10.5194/gmd-12-4375-2019, 2019.

Jones, C. and Friedlingstein, P. Quantifying process-level uncertainty contributions to TCRE and Carbon Budgets for meeting Paris Agreement climate targets. Environmental Research Letters. 15. 10.1088/1748-9326/ab858a, 2020.

Kanter, D.R., Winiwarter, W., Bodirsky, B.L., Bouwman, L., Boyer, E., Buckle, S., Compton, J.E., Dalgaard, T., de Vries, W., Leclere, D., Leip, A., Müller, C., Popp, A., Raghuram, N., Rao, S., Sutton, M.A., Tian, H., Westhoek, H., Zhang, X., and Zurek, M.: Nitrogen futures in the shared socioeconomic pathways 4, Glob Environ Change, 61, 102029. doi: 10.1016/j.gloenvcha.2019.102029. PMID: 32601516; PMCID: PMC7321850, 2020.

Kawamiya, M., Hajima, T., Tachiiri, K., Watanabe, S. and Yokohata, T.: Two decades of Earth system modeling with an emphasis on Model for Interdisciplinary Research on Climate (MIROC), Prog Earth Planet Sci 7, 64, https://doi.org/10.1186/s40645-020-00369-5, 2020.

Lamboll, R.D., Nicholls, Z.R.J., Smith, C.J. et al. Assessing the size and uncertainty of remaining carbon budgets. Nat. Clim. Chang. 13, 1360–1367, https://doi.org/10.1038/s41558-023-01848-5, 2023.

Loozen, Y., Rebel, K., De Jong, S., Lu, M., Ollinger, S., Wassen, M. and Karssenberg, D. Mapping canopy nitrogen in European forests using remote sensing and environmental variables with the random forests method. Remote Sensing of Environment. 247. 111933. 10.1016/j.rse.2020.111933, 2020.

Lu, C., and Tian, H.: Global nitrogen and phosphorus fertilizer use for agriculture production in the past half century: Shifted hot spots and nutrient imbalance, Earth System Science Data, 9, 181-192. https://doi.org/10.5194/essd-9-181-2017, 2017.

MacDougall, A. H., Avis, C. A., and Weaver, A. J.: Significant contribution to climate warming from the permafrost carbon feedback, Nat. Geosci., 5, 719–721, 2012.

MacDougall, A. H., Zickfeld, K., Knutti, R. and Matthews, D. Sensitivity of carbon budgets to permafrost carbon feedbacks and non-CO2 forcings. Environ. Res. Lett. 11 019501, http://dx.doi.org/10.1088/1748-9326/11/1/019501, 2015.

MacDougall, A. H. and Knutti, R.: Projecting the release of carbon from permafrost soils using a perturbed parameter ensemble modelling approach, Biogeosciences, 13, 2123–2136, https://doi.org/10.5194/bg-13-2123-2016, 2016.

MacDougall, A.H. The Transient Response to Cumulative CO2 Emissions: a Review. Curr Clim Change Rep 2, 39–47, https://doi.org/10.1007/s40641-015-0030-6, 2016.

MacDougall, A. H., Swart, N. C., and Knutti, R. The Uncertainty in the Transient Climate Response to Cumulative CO2 Emissions Arising from the Uncertainty in Physical Climate Parameters, Journal of Climate, 30(2), 813-827, 2017.

MacDougall, A. H.: Limitations of the 1% experiment as the benchmark idealized experiment for carbon cycle intercomparison in C4MIP, Geosci. Model Dev., 12, 597–611, https://doi.org/10.5194/gmd-12-597-2019, 2019.

MacDougall, A. H., Frölicher, T. L., Jones, C. D., Rogelj, J., Matthews, H. D., Zickfeld, K., Arora, V. K., Barrett, N. J., Brovkin, V., Burger, F. A., Eby, M., Eliseev, A. V., Hajima, T., Holden, P. B., Jeltsch-Thömmes, A., Koven, C., Mengis, N., Menviel, L., Michou, M., Mokhov, I. I., Oka, A., Schwinger, J., Séférian, R., Shaffer, G., Sokolov, A., Tachiiri, K., Tjiputra , J., Wiltshire, A., and Ziehn, T.: Is there warming in the pipeline? A multi-model analysis of the Zero Emissions Commitment from CO2, Biogeosciences, 17, 2987–3016, https://doi.org/10.5194/bg-17-2987-2020, 2020.

MacDougall, A. H.: Estimated effect of the permafrost carbon feedback on the zero emissions commitment to climate change, Biogeosciences, 18, 4937–4952, https://doi.org/10.5194/bg-18-4937-2021, 2021.

Matthews, H. D., Gillett, N., Stott, P., and Zickfeld, K.: The proportionality of global warming to cumulative carbon emissions, Nature, 459, 829-832. https://doi.org/10.1038/nature08047, 2009.

Matthews, H. D., Tokarska, K., Nicholls, Z.R.J., Rogelj, J., Canadell, Josep, Friedlingstein, P., Frölicher, Thomas, Forster, Piers, Gillett, Nathan, Ilyina, T., Jackson, R., Jones, Chris, Koven, C., Knutti, R., MacDougall, A.H., Meinshausen, M., Mengis, N., Séférian, R., and Zickfeld, K.: Opportunities and challenges in using remaining carbon budgets to guide climate policy, Nature Geoscience, 13. https://doi.org/10.1038/s41561-020-00663-3, 2020.

McGill, W., Cole, C.: Comparative aspects of cycling of organic C, N, S, and P through soil organic matter.Geoderma 26, 267–286, 1981.

Meissner, K. J., Weaver, A. J., Matthews, H. D., and Cox, P. M.: The role of land surface dynamics in glacial inception: a study with the UVic Earth System Model, Clim. Dynam., 21, 515–537, https://doi.org/10.1007/s00382-003-0352-2, 2003.

Menge D., Hedin, L., Pacala S.: Nitrogen and Phosphorus Limitation over Long-Term Ecosystem Development in Terrestrial Ecosystems, PLOS ONE 7(8), https://doi.org/10.1371/journal.pone.0042045, 2012.

Mengis, N., Partanen, A.-I., Jalbert, J., and Matthews, H. D.: 1.5 °C carbon budget dependent on carbon cycle uncertainty and future non-CO2 forcing, Scientific Reports, 8, 5831. https://doi.org/10.1038/s41598-018-24241-1, 2018.

Mengis, N., Keller, D. P., MacDougall, A. H., Eby, M., Wright, N., Meissner, K. J., Oschlies, A., Schmittner, A., MacIsaac, A. J., Matthews, H. D., and Zickfeld, K.: Evaluation of the University of Victoria Earth System Climate Model version 2.10 (UVic ESCM 2.10), Geosci. Model Dev., 13, 4183–4204, https://doi.org/10.5194/gmd-13-4183-2020, 2020.

Myhre, G., Stocker, F., Qin, D., Plattner, G, Tignor,M., Allen, S., Boschung, J., Nauels, A., Xia, Y., Bex, V. and Midgley, P.: Anthropogenic and natural radiative forcing. Working Group I Contribution to the Intergovernmental Panel on Climate Change Fifth Assessment Report Climate Change 2013: The Physical Science Basis, Eds., Cambridge University Press, 2013.

Nakhavali, M., Mercado, L., Hartley, I., Sitch, S., Cunha, F., di Ponzio, R., Lugli, L., Quesada, C., Andersen, K., Chadburn, S., Wiltshire, A., Clark, D., Ribeiro, G., Siebert, L., Moraes, A., Schmeisk Rosa, J., Assis, R., and Camargo, J. L.: Representation of phosphorus cycle in Joint UK Land Environment Simulator (vn5.5JULES-CNP), Geosci. Model Dev. Discuss., https://doi.org/10.5194/gmd-2021-403, 2021.

Brian C. O'Neill, Elmar Kriegler, Kristie L. Ebi, Eric Kemp-Benedict, Keywan Riahi, Dale S. Rothman, Bas J. van Ruijven, Detlef P. van Vuuren, Joern Birkmann, Kasper Kok, Marc Levy, William Solecki: The roads ahead: Narratives for shared socioeconomic pathways describing world futures in the 21st century, Global Environmental Change,volume 42:169-180, https://doi.org/10.1016/j.gloenvcha.2015.01.004, 2017.

Pacanowski, R. C.: MOM 2 Documentation, users guide and reference manual, GFDL Ocean Group Technical Report 3, Geophys, Fluid Dyn. Lab., Princet. Univ. Princeton, NJ, 1995.

Palazzo-Corner, S., Siegert, M., Ceppi, P., Fox-Kemper, B., Frölicher, T.L., Gallego-Sala, A., Haigh, J., Hegerl, G.C., Jones, C.D., Knutti, R., Koven, C.D., MacDougall, A.H., Meinshausen, M., Nicholls, Z., Salle´ e, J.B., Sanderson, B.M., Se´ fe´ rian, R., Turetsky, M., Williams, R.G., Zaehle, S. and Rogelj, J. The Zero Emissions Commitment and climate stabilization, Front Sci, 1:117074, doi: 10.3389/fsci.2023.1170744. 2023.

Popp, J., Lakner, Z., Harangi-Rákos, M. and Fári, M. The effect of bioenergy expansion: Food, energy, and environment, Renewable and Sustainable Energy Reviews, 32:559-578, https://doi.org/10.1016/j.rser.2014.01.056, 2014.

Reed, S. C., Townsend, A. R., Davidson, E. A., and Cleveland, C.: Stoichiometric patterns in foliar nutrient resorption across multiple scales. New Phytol. 196, 173–180, doi: 10.1111/j.1469-8137.2012.04249, 2012.

Rogelj, J., Shindell, D., Jiang, K., Fifita, S., Forster, P., Ginzburg, V., Handa, C., Kheshgi, H., Kobayashi, S., Kriegler, E., Mundaca, L., Séférian, R., and Vilariño, M.V. (In Press): Mitigation pathways compatible with 1.5°C in the context of sustainable development. In Global warming of 1.5°C. An IPCC Special Report on the impacts of global warming of 1.5°C above pre-industrial levels and related global greenhouse gas emission pathways, in the context of strengthening the global response to the threat of climate change, sustainable development, and efforts to eradicate poverty [V. Masson-Delmotte, P. Zhai, H. O. Pörtner, D. Roberts, J. Skea, P. R. Shukla, A. Pirani, W. Moufouma-Okia, C. Péan, R. Pidcock, S. Connors, J.B.R. Matthews, Y. Chen, X. Zhou, M.I. Gomis, E. Lonnoy, T. Maycock, M. Tignor, T. Waterfield (eds.)], 2018.

Spafford, L. and Macdougall, A.H.: Quantifying the probability distribution function of the transient climate response to cumulative CO2 emissions. Environmental Research Letters. 15. 10.1088/1748-9326/ab6d7b, 2020.

Spafford, L., and Macdougall, A.H.: Quantifying the probability distribution function of the transient climate response to cumulative CO2 emissions, Environmental Research Letters, 15. https://doi.org/10.1088/1748-9326/ab6d7b, 2020.

Thornton, P., Lamarque, J., Rosenbloom, N., and Mahowald, N.: Influence of carbon-nitrogen cycle coupling on land model response to CO_2 fertilization and climate variability, Global Biogeochem. Cycles 21, doi:10.1029/2006GB002868, 2007.

Selman, M., Greenhalgh, S., Diaz, R. and Sugg, Z.: Eutrophication and hypoxia in coastal areas: a global assessment of the state of knowledge. WRI Policy Note. 1-6, 2008.

Seitzinger, S. P., Mayorga, E., Bouwman, A. F., Kroeze, C., Beusen, A. H. W., Billen, G., Van Drecht, G., Dumont, E., Fekete, B. M., Garnier, J., and Harrison, J. A.: Global river nutrient export: A scenario analysis of past and future trends, Global Biogeochem. Cy., 24, GB0A08, doi:10.1029/2009GB003587, 2010.

Shibata, H., Branquinho, C., McDowell, W. H., Mitchell, M. J., Monteith, D. T., Tang, J., Arvola, L., Cruz, C., Cusack, D. F., Halada, L., Kopáček, J., Máguas, C., Sajidu, S., Schubert, H., Tokuchi, N., and Záhora, J.: Consequence of altered nitrogen cycles in the coupled human and ecological system under changing climate: The need for long-term and site-based research. Ambio, 44(3), 178–193, https://doi.org/10.1007/s13280-014-0545-4, 2015.

Smil, V.: Phosphorus in the environment: natural flows and human interferences, Annual Review of Energy and Environment, 25,53–88, 2000.

Tokarska, K., Gillett, N., Arora, V., Lee, W., and Zickfeld, K. (2018). The influence of non-CO2 forcings on cumulative carbon emissions budgets. Environmental Research Letters, 13. https://doi.org/10.1088/1748-9326/aaafdd, 2018.

Walker, A., Beckerman, A., Gu, L., Kattge, J., Cernusak, L., Domingues, T., Scales, J., Wohlfahrt, G., Wullschleger, S. and Woodward, I.: The relationship of leaf photosynthetic traits - Vcmax and Jmax - to leaf nitrogen, leaf phosphorus, and specific leaf area: A meta-analysis and modeling study, Ecology and Evolution, 4, 2014.

Wania, R., Meissner, K., Eby, M., Arora, V., Ross, I., and Weaver, A.: Carbon-nitrogen feedbacks in the UVic ESCM, Geosci. Model Dev., 5, 1137–1160, https://doi.org/10.5194/gmd-5-1137-2012, 2012.

Wang, Y., Houlton, B., Field, C.: A model of biogeochemical cycles of carbon, nitrogen, and phosphorus including symbiotic nitrogen fixation and phosphatase production. Global Biogeochemical Cycles 21, 2007.

Wang, Y., Law, R., Pak, B.: A global model of carbon,nitrogen and phosphorus cycles for the terrestrial biosphere, Bio-geosciences 7, 2261–2282,doi:10.5194/bg-7-2261-2010, 2010.

Wang, Y. and Goll, D.: Modelling of land nutrient cycles: recent progress and future development, Faculty Reviews. 10. 10.12703/r/10-53.

Wang, Y., Zhang, Q., Pitman, A. and Dai, Y. Nitrogen and phosphorous limitation reduces the effects of land use change on land carbon uptake or emission. Environmental research letters, 10 (2015) 014001, http://dx.doi.org/10.1088/1748-9326/10/1/014001, 2015.

Wei, N., Xia, J., Wang, Y. P., Zhang, X., Zhou, J., Bian, C., and Luo, Y. Nutrient limitations lead to a reducedmagnitude of disequilibrium in theglobal terrestrial carbon cycle. Journal ofGeophysical Research: Biogeosciences,127, e2021JG006764. https://doi.org/10.1029/2021JG006764, 2022.

Weaver, A. J., Eby, M., Wiebe, E. C., Bitz, C. M., Duffy, P. B., Ewen, T. L., Fanning, A. F., Holland, M. M., MacFadyen, A., Matthews, H. D., Meissner, K. J., Saenko, O., Schmittner, A., Wang, H. X., and Yoshimori, M.: The UVic Earth System Climate Model: Model description, climatology, and applications to past, present and future climates, Atmos. Ocean, 39, 361–428, 2001.

Wieder, W., Cleveland, C., Smith, W. and Todd, K.: Future productivity and carbon storage limited by terrestrial nutrient availability, Nature Geosci 8, 441–444, https://doi.org/10.1038/ngeo2413, 2015.

van Puijenbroek, P., Beusen, A. and Bouwman, A.: Global nitrogen and phosphorus in urban waste water based on the Shared Socio-economic pathways, Journal of Environmental Management, 231: 446-456, https://doi.org/10.1016/j.jenvman.2018.10.048, 2019.

Zickfeld, K., Eby, M., Matthews, H. D., and Weaver, A. J.: Setting cumulative emissions targets to reduce the risk of dangerous climate change, Proceedings of the National Academy of Sciences, 106, 16 129–16 134, 2009.